Low-Temperature, Nontoxic Water-Induced Metal-Oxide Thin Films and Their Application in Thin-Film Transistors

Guoxia Liu, Ao Liu, Huihui Zhu, Byoungchul Shin, Elvira Fortunato, Rodrigo Martins, Yiqian Wang, and Fukai Shan**

Here, a simple, nontoxic, and inexpensive "water-inducement" technique for the fabrication of oxide thin films at low annealing temperatures is reported. For water-induced (WI) precursor solution, the solvent is composed of water without additional organic additives and catalysts. The thermogravimetric analysis indicates that the annealing temperature can be lowered by prolonging the annealing time. A systematic study is carried out to reveal the annealing condition dependence on the performance of the thin-film transistors (TFTs). The WI indium-zinc oxide (IZO) TFT integrated on SiO_2 dielectric, annealed at 300 °C for 2 h, exhibits a saturation mobility of 3.35 $cm^2 V^{-1} s^{-1}$ and an on-to-off current ratio of ≈10^8. Interestingly, through prolonging the annealing time to 4 h, the electrical parameters of IZO TFTs annealed at 230 °C are comparable with the TFTs annealed at 300 °C. Finally, fully WI IZO TFT based on YO_x dielectric is integrated and investigated. This TFT device can be regarded as "green electronics" in a true sense, because no organic-related additives are used during the whole device fabrication process. The as-fabricated IZO/YO_x TFT exhibits excellent electron transport characteristics with low operating voltage (≈1.5 V), small subthreshold swing voltage of 65 mV dec^{-1} and the mobility in excess of 25 $cm^2 V^{-1} s^{-1}$.

1. Introduction

Amorphous metal-oxide semiconductors have been extensively studied as the channel material for thin-film transistors (TFTs) in display backplanes and other optoelectronic devices.[1] Recently, the semiconducting thin films, including indium oxide (In_2O_3), indium-zinc oxide (IZO), gallium-zinc-tin oxide, and indium-gallium-zinc oxide (IGZO), moved into the focus of current research because of their high mobility, high transparency, and large-area uniformity.[1d,1e,2] The research of electronic devices fabricated via solution process has been regarded as a key part of next-generation low-cost and sustainable processing methods. For this reason, considerable researches have been conducted on the development of spin coating, spray pyrolysis, screen printing, and ink jet printing for the construction of metal-oxide TFTs. In most of the previous reports of solution-processed TFTs, high-temperature annealing process is imperative to achieve reasonable electrical properties of the devices. To decrease the annealing temperature of solution-processed metal oxide, several researchers have ever proposed novel approaches, including sol-gel on chip,[1e] chemical energetic combustion process through an oxidizer and fuel,[1d,3] and UV/ozone photo-annealing method[4] to achieve oxide TFTs at temperatures under 300 °C. However, the inert atmosphere is necessary to handle precursor solutions, which makes the experiment complicated. Furthermore, the toxic organic solvents, e.g., 2-methoxyethanol (2-ME) and dimethyl formamide, are usually used. Additional additives or follow-up processing steps undoubtedly increase the environmental damage and the fabrication cost. To develop an eco-friendly synthetic route, aqueous zinc hydroxo-amine complex precursor was proposed to fabricate the channel layer of TFTs.[5] However, these precursors are highly sensitive to potential of hydrogen (PH) value and the tendency to form ZnO nuclei leading to sedimentation is increased by utilizing ammonium hydroxide.[6] In addition, time-consuming and cumbersome processes for complex precipitation steps cause considerable deviation when preparing the precursor, which may induce variation in electrical performance of the metal oxide TFTs.

In consideration of sustainable benefits and strong potential of the solution-based process, the eco-friendly and organic-species-free precursors are needed in the future display industry. As a solvent, water meets the current environmental awareness restricting the use of ecologically harmful substances and process. Instead of the often used organic-based solvents, the water-induced (WI) synthesis is considered to be healthier, safer and environmentally friendlier. Besides the absence of hazardous solvents, the simple and inexpensive synthesis

Dr. G. X. Liu, A. Liu, H. H. Zhu, Dr. Y. Q. Wang, Prof. F. K. Shan
College of Physics and Lab of New Fiber Materials and Modern Textile
Growing Base for State Key Laboratory
Qingdao University
Qingdao 266071, P.R. China
E-mail: gxliu@qdu.edu.cn; fkshan@gmail.com
Dr. B. C. Shin
Electronic Ceramics Center
Dong-Eui University
Busan 614-714, Korea
Dr. E. Fortunato, Dr. R. Martins
Department of Materials Science/CENIMAT-I3N, Faculty of Sciences and Technology
New University of Lisbon and CEMOP-UNINOVA
Campus de Caparica
2829-516 Caparica, Portugal

DOI: 10.1002/adfm.201500056

© 2015 WILEY-VCH Verlag GmbH & Co. KGaA, Weinheim

and decomposition equipment is an additional asset. Unlike conventionally used precursors, the WI solutions are insensitive to ambient moisture. Therefore, an inert atmosphere to store and handle precursor solutions is not necessary.[7] More importantly, as the coordinating bond between metal cation and neighboring aquo ion is relatively weak (electrostatic interaction), it is easily broken with low thermal energy compared with the covalent bonds in organic-based precursors.[2a] Therefore, WI synthetic process is considered to be a promising technique to fabricate metal-oxide dielectric and channel layers for eco-friendly TFTs at low temperature.

It has been proved that the carrier concentration and transport properties of metal-oxide thin films from molecular precursor solutions strongly depend on the preparation conditions, in particular on the annealing temperature and, to some surprise, also on the concentration of the precursor solution.[1d,1e,2a,8] However, there is few reports discussing the annealing time effects on the electrical performance of the oxide TFTs. Choi et al. reported the IGZO TFTs using a sol–gel process and studied the annealing time effects (from 1 to 12 h) on the electrical performance of the TFTs.[9] In their report, 2-ME and monoethanolamine were used as the solvent and the stabilizer, respectively. Unfortunately, very small difference was investigated from the transfer characteristics of the TFTs with various annealing time. For the conventional organic-based precursor solution, a constant thermal energy is needed to break the chemical bond existed in the specific organic species. The degree of oxide-lattice formation and oxygen-vacancy generation depends, for a given composition, primarily on the annealing temperature.[10] However, for WI precursor, the high thermal energy is not necessary due to the simple electrostatic interaction between the metal cation and the hydroxide species. A relatively long annealing time at low temperature is expected to achieve the same effects of the dehydroxylation and the alloy reaction instead of the requirement of high temperature annealing process.

In this report, nontoxic solution-processed metal-oxide channel and dielectric layers were fabricated using WI synthesis method at low temperatures. For WI precursor solutions, the thermogravimetric analysis (TGA) indicates that the annealing temperature can be lowered by prolonging the annealing time. Based on this phenomenon, an in-depth investigation was conducted to reveal the effects of annealing time on metal-oxide thin film formation and on the performance of the TFTs. Finally, the fully WI amorphous IZO TFT based on YO_x dielectric was integrated. The high-k YO_x dielectric was first synthesized using WI process and exhibited acceptable dielectric and electrical performance. Meanwhile, the as-fabricated IZO/YO_x TFT successfully operated as a switching device at an ultralow operating voltage of 1.5 V.

2. Results and Discussion

2.1. Properties of WI Precursor Solutions

The combination of metal nitrates and water as the precursors and solvent provides a simple and unique structure in solution state. Water is a frequently used solvent with a high static dielectric constant of ≈80 at room temperature, which favors the dissociation of ionic species and acts as the σ-donor molecule that reacts as a nucleophilic ligand.[7] When the metal nitrates was dissolved in water, the m^{n+} are solvated by the neighboring water molecules. In this work, IZO ternary system was chosen as the channel layer because of its high mobility even in the amorphous state, the high transparency in the visible region, and fewer electron scattering centers in the lattice than a quaternary semiconductor system.[2b,3] In the case of divalent and trivalent first row transition cations, these hydrated cations can be considered as true coordination complexes with six water molecules acting as σ-donating ligands.[7] Meanwhile, as the coordination number of In^{3+} is 6, both of Zn^{2+} and In^{3+} can be considered as true coordination complexes with six water molecules. The schematic representation of zinc and indium complex in water solution was shown in Figure S1, Supporting Information.

2.2. TGA of WI IZO Xerogel

To understand the formation of oxide thin films from WI precursor, TGA analysis of IZO xerogel was performed and the results are shown in **Figure 1**. At the early stage of the annealing process, thermally driven hydrolysis occurred. With increasing the annealing temperature further, the dehydroxylation and alloy reaction via olation (Equation (1)) and oxolation (Equations (2) and (3)) occurred, which were based on a nucleophilic reaction between metal cations.[2a,11] The relatively large difference of electronegativity (χ) between In (χ = 1.78) and Zn (χ= 1.65) facilitates the condensation reaction and results in a low level of hydroxide-related species. In addition, the partial charge of oxygen participate in the nucleophilic reaction due to

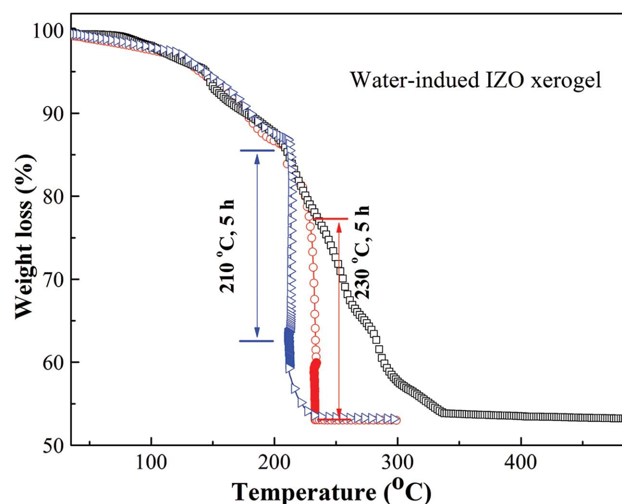

Figure 1. TGA curves of WI IZO precursor annealed at various conditions. The black (squares) line: annealed from 50 to 500 °C with heating rate of 10 °C min^{-1} in the air; the blue (triangles) line include three steps: I) annealed from 50 to 210 °C with heating rate of 10 °C min^{-1}, II) kept at 210 °C for 5 h, and III) annealed from 210 to 300 °C with heating rate of 10 °C min^{-1}; the red (circles) line include three steps: I) annealed from 50 to 230 °C with heating rate of 10 °C min^{-1}, II) kept at 230 °C for 5 h, and III) annealed from 230 to 300 °C with heating rate of 10 °C min^{-1}.

© 2015 WILEY-VCH Verlag GmbH & Co. KGaA, Weinheim

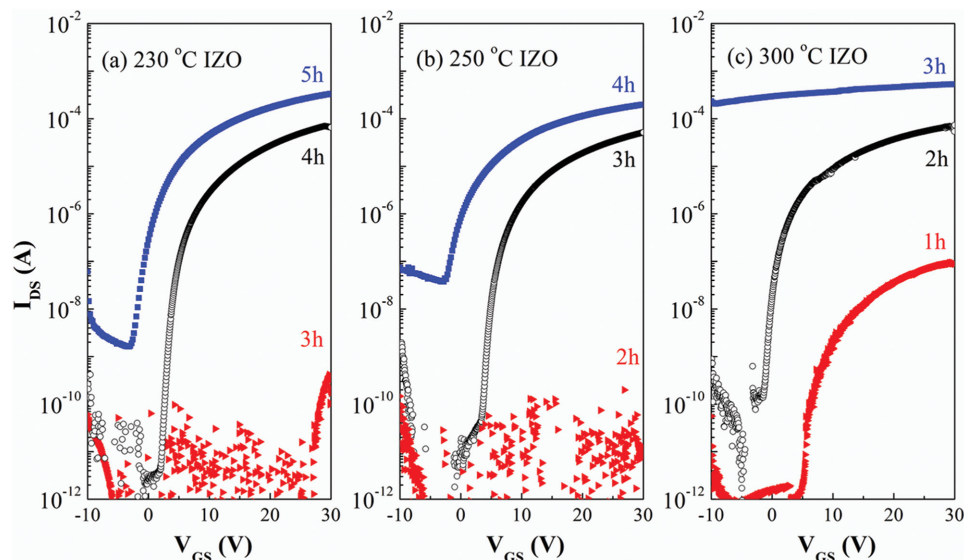

Figure 2. Transfer curves of IZO TFTs annealed at various conditions. The source-drain voltage (V_{DS}) was 15 V.

the larger difference in electronegativity (χ_{oxygen} = 3.44). Since the oxolation reaction, which eliminates the H and completes the oxide formation in the reaction, is achieved by a nucleophilic reaction, more negative partial charge of oxygen in OH stimulates the nucleophilic reaction and results in a lower level of OH species.

$$M_1{-}OH + M_2{-}OH_2 \rightarrow M_1{-}OH{-}M_2 + H_2O \quad (1)$$

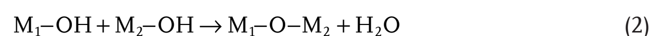

$$M_1{-}OH + M_2{-}OH \rightarrow M_1{-}O{-}M_2 + H_2O \quad (2)$$

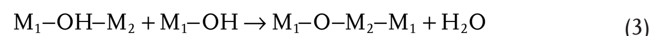

$$M_1{-}OH{-}M_2 + M_1{-}OH \rightarrow M_1{-}O{-}M_2{-}M_1 + H_2O \quad (3)$$

For conventional organic-based precursor route, reasonable device performance is typically achievable for annealing temperatures greater than that of metal-oxide lattice formation or organic impurity oxidation.[12] As a consequence, the annealing temperature for metal-oxide thin films was usually higher than the final decomposition temperature determined by TGA analysis. However in WI system, simple electrostatic interaction existed in water-based precursors, a lower annealing temperature with sufficient annealing time is expected to achieve the dehydroxylation and condensation processes. Instead of continuous annealing process up to 500 °C, the IZO xerogel was annealed at 210 °C and 230 °C for 5 h, respectively. Interestingly, it can be clearly seen that the weights of IZO xerogel were gradually decreased during annealing retaining process. A sequential weight loss was observed for 210 °C-annealed IZO xerogel when the temperature was increased further. While the weight of the 230 °C-annealed IZO xerogel kept unchanged, and the final weight loss percentage was equal to that of the IZO xerogel calcined up to 500 °C. From the TGA results, it is easily understood that low-temperature annealing for WI IZO precursor in a long period can achieve the dehydroxylation rather than the annealing process at much higher temperature. The alloy reaction during this period will be discussed in detail later.

2.3. Electrical Properties of WI IZO and In_2O_3 TFTs

Based on the aforementioned TGA results, a systematic study of the WI oxide thin films was carried out by combining the application in TFT devices. The performance of the as-fabricated TFTs was assessed through the analysis of the field-effect mobility (μ_{FE}), threshold voltage (V_{TH}), and thermal activation energy for carrier transport. **Figure 2**a–c show the representative transfer characteristics for TFTs based on WI IZO channel layers. The TFT parameters, as the function of the annealing time, are summarized in **Table 1**. It is found that the μ_{FE} increases with increasing annealing time, independent of annealing temperature. Meanwhile, the operation mode of the TFTs was changed from enhancement mode to depletion mode. When the annealing temperature was kept at 300 °C, it can be clearly seen that the electrical properties of the 300 °C-annealed IZO TFTs for 2 h showed the best performance, including a reasonable μ_{FE} of 3.35 cm^2 V^{-1} s^{-1}, a high on/off current ratio (I_{on}/I_{off}) of 6 × 10^7, and a low V_{TH} of 1.5 V. Interestingly, at an

Table 1. Electrical parameters of WI IZO TFTs annealed at various conditions.

T_a [°C]	Time [h]	μ_{FE} [cm^2 V^{-1} s^{-1}]	V_{TH} [V]	I_{on}/I_{off}
210		Inactive (TFT always off)		
230	3	Inactive (TFT always off)		
	4	2.79	3.2	6.0×10^7
	5	5.21	−0.3	6.5×10^5
250	2	Inactive (TFT always off)		
	3	3.12	2.3	5.8×10^7
	4	4.85	−1.6	5.0×10^3
300	1	–	11.0	9.0×10^4
	2	3.35	1.5	6.0×10^7
	3	Conductive (TFT always on)		

© 2015 WILEY-VCH Verlag GmbH & Co. KGaA, Weinheim

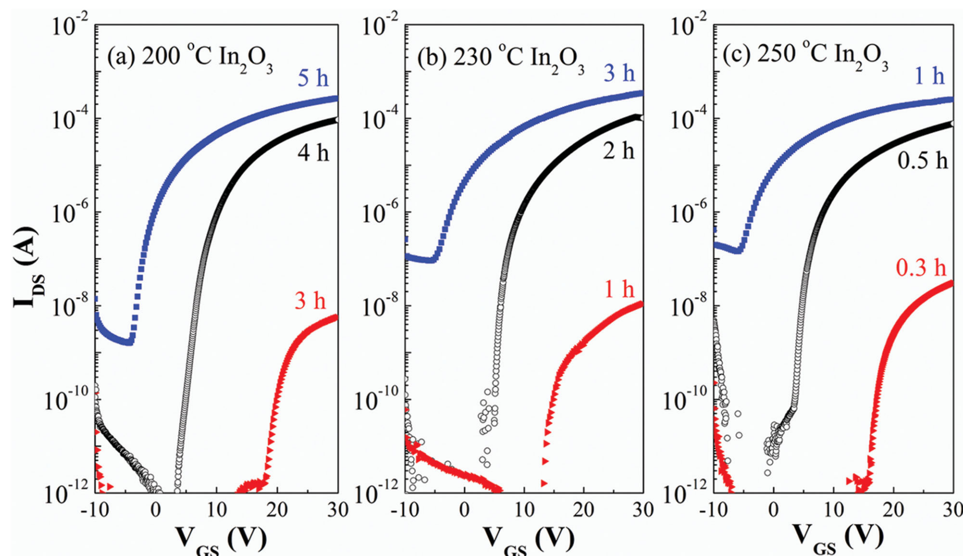

Figure 3. Transfer curves of WI In_2O_3 TFTs annealed at various conditions. The V_{DS} was 15 V.

annealing temperature of 230 °C by increasing the annealing time from 2 to 4 h, the devices are activated, working in the enhancement, with a good saturation mobility and a high on/off ratio, which matches well with the thermal analysis performed. Compared with the previous literatures based on conventional organic-based approach, the WI synthesis route allows for the preparation of IZO TFTs at lower annealing temperatures.[12,13]

Meanwhile, we analyzed the effects of the annealing time on the performance of the WI In_2O_3 TFTs annealed at various temperatures. The corresponding transfer characteristics of the TFTs are shown in **Figure 3**a–c, which presents similar trends with IZO TFTs. The key parameters are summarized in Table S1, Supporting Information. It is known that the carrier concentration of In_2O_3 channel layer can be modulated by the addition of various metal cations, that is, Zn, Ga, and Al. Therefore, a relatively low thermal-driven energy is needed for In_2O_3 channel layer compared with IZO layer. Based on the results of the IZO and In_2O_3 layers annealed at various conditions, it can be concluded that the formation of metal-oxide thin films by using water as the solvent is promising for low-temperature processed devices.

2.4. Analysis of X-Ray Photoelectron Spectroscopy (XPS) Results for WI IZO Thin Films

To understand the mechanism of the electrical performance as function of annealing time, the chemical states of the IZO thin films with various annealing time were analyzed by XPS and are shown in **Figure 4**a, b. All the XPS peaks are calibrated by taking C 1s reference at 284.8 eV to compensate for any charge-induced shift. The O 1s of the XPS spectrum was fitted by a Gaussian distribution, which could be divided into three peaks centered at 529.7, 531.2, and 531.9 eV, respectively. The peak centers at 529.7 and 531.2 eV can be assigned to the oxygen in oxide lattices (M—O—M) and oxygen vacancy in lattices (V_O), respectively.[10] The feature at 531.9 eV can be assign to the bonded oxygen in hydroxide-related (M—OH) species. Since H is more electronegative than the metals (In and Zn), the M—OH oxygen atoms are less negatively charged than those in oxides, shifting the XPS feature toward higher binding energy. The semiquantitative analyses of oxygen compositions are shown in Figure 4c, d. The atomic percentages were calculated based on the area integration of each O 1s peak. Note that the IZO thin films annealed at 230 °C for 3 h are primarily composed of hydroxides, which indicates that the intermediate compounds do not undergo transformation into metal oxides. This is in good agreement with the IZO TFTs not being electrically active at 230 °C for 3 h. In contrast, IZO thin films annealed at 230 °C with longer annealing time exhibit a decreased content of M—OH and the increased fraction of M—O—M and V_O species. Similarly, the same tendency was observed in 300 °C-annealed IZO thin films. This phenomenon is mainly because that the M—OH bonds are gradually converted into the M—O—M bonds via thermal-driven condensation processes by prolonging the annealing time at the same temperature.

It is known that the conduction band minimum in metal-oxide semiconductors is primarily composed of dispersed vacant s-states with short interaction distances for efficient carrier transport, which can be achieved in ionic oxide but not obviously in hydroxide. Therefore, it is reasonable that M—O—M bonding formation is essential prerequisite for low-temperature-processed semiconducting thin films with acceptable electrical performance. These results are consistent with the aforementioned observations that the mobilities of WI IZO TFTs increase with increasing annealing time at a fixed annealing temperature.

The V_O formation is closely related to the charge carrier generation. With prolonging the annealing time, enhanced V_O formation generated higher intrinsic carrier concentration in IZO channel layer, which led to a higher mobility and a negative shift in V_{TH} of TFT devices. Park et al. have ever proposed that a high-performance metal-oxide semiconductor needs

© 2015 WILEY-VCH Verlag GmbH & Co. KGaA, Weinheim

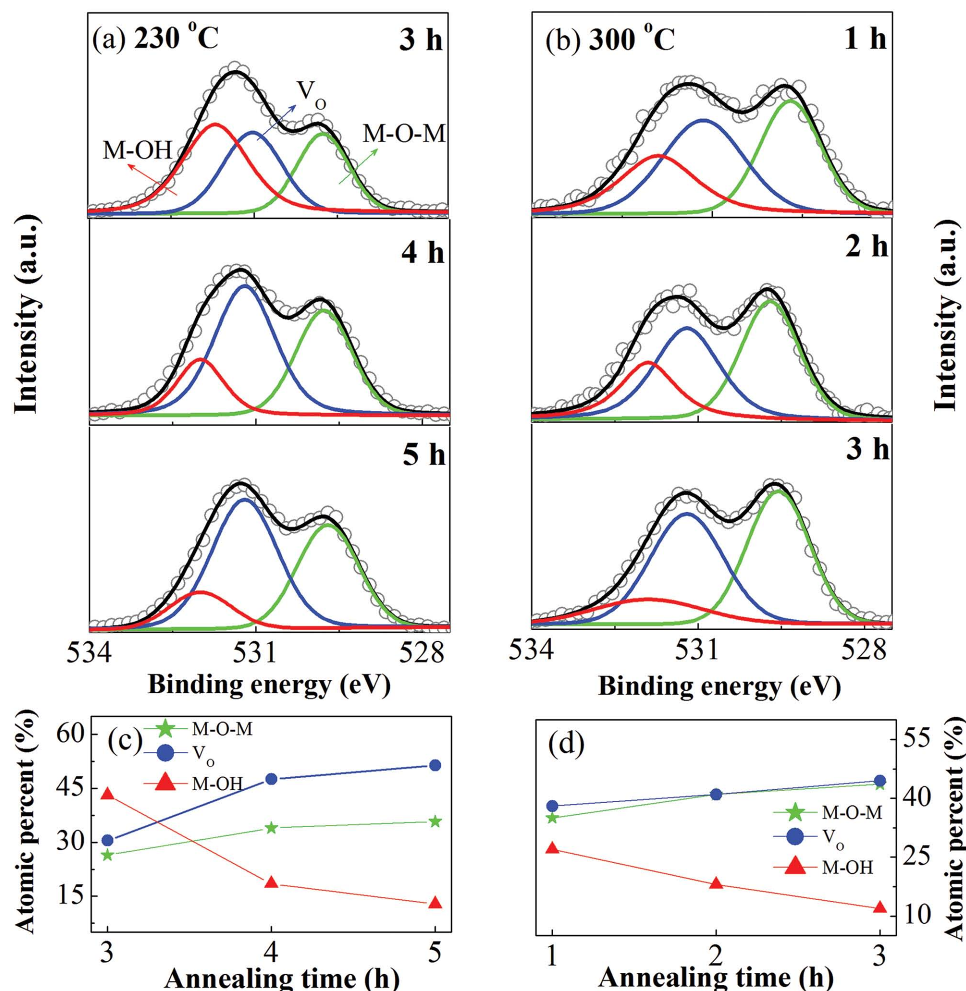

Figure 4. a,b) XPS O1s spectra of IZO thin films annealed at the indicated conditions. c,d) Semiquantitative analyses of the oxygen component for the corresponding IZO thin films.

a proper ratio between oxygen deficiency and metal oxide lattice.[5b] Although the ratio of V_O to M—O—M is somewhat controversial in this work, the same ratio variation gives the information to explain the property dependence on annealing time.

2.5. Uniformity Characteristics of IZO TFT Devices

Device uniformity is substantial important for the practical applications for TFT devices. To investigate the uniformity of WI TFT devices, 20 TFT units (4 × 5 array) were separately fabricated and annealed at 230 °C for various time. Statistical data for 4 h-annealed IZO TFTs show devices with an average μ_{FE} of 2.89 $cm^2 V^{-1} s^{-1}$ (σ = 0.38) and turn-on voltage of –1.14 V (σ = 0.65), which are shown in **Figure 5**a,b. The corresponding transfer curves of the 20 TFTs are shown in Figure S2, Supporting Information. It is noted that a few devices exhibited higher μ_{FE} (3.1–3.3 $cm^2 V^{-1} s^{-1}$), which were quite close to the IZO TFTs fabricated at 300 °C for 2 h. Meanwhile, the 5 h-annealed IZO TFTs also exhibit acceptable device uniformity with an average μ_{FE} of 5.17 $cm^2 V^{-1} s^{-1}$ (σ = 0.21) and turn-on voltage of –3.9 V (σ = 0.54), as shown in Figure S3, Supporting Information.

2.6. Electrical and Structural Properties of WI YO_x Dielectric

To investigate the possibility of improved features of the WI IZO TFTs based on high-*k* dielectric, the YO_x thin film was fabricated by solution process and the IZO TFT based on YO_x dielectric was also integrated. In our previous report, fully solution-processed In_2O_3/ZrO_x TFTs were achieved and exhibited satisfied electrical performance.[14] However in that work, the ZrO_x dielectric was synthesized through organic-based approach, which is not good for the environment protection and sustainable development. To solve this problem, we firstly propose an eco-friendly WI process to fabricate the high-*k* YO_x dielectric. The fully WI IZO/YO_x TFT is a true sense of "green electronics," in which no any organic-related additives in the whole device fabrication processes was involved.

In general, high-*k* dielectrics, such as ZrO_x,[15] AlO_x,[16] YO_x,[17] HfO_x,[18], or multiband gap strucutres [19] bring about an increase in μ_{FE} due to the excellent heterogeneous interface

© 2015 WILEY-VCH Verlag GmbH & Co. KGaA, Weinheim

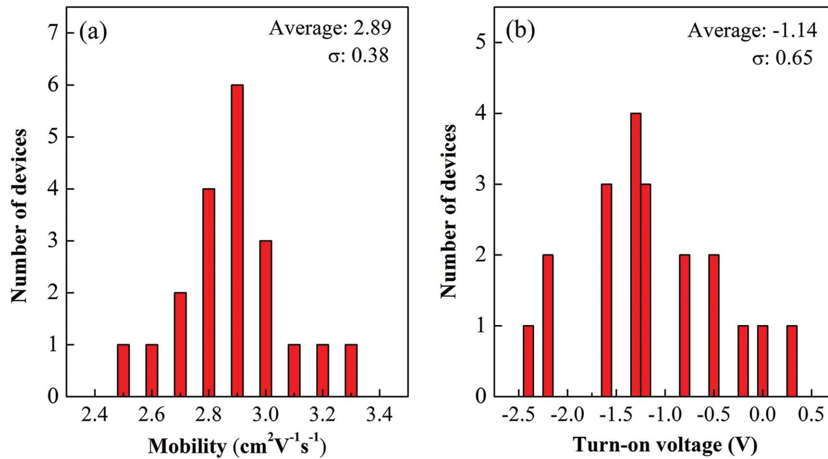

Figure 5. Histogram of the a) mobility and b) turn-on voltage for IZO TFTs (4 × 5 array) processed at 230 °C for 4 h. σ represents the standard deviation.

layer formed with metal-oxide semiconductors.[15,20] In addition, the mobility of the carriers in the semiconductor layer is strongly dependent on the carrier concentration, which is mainly determined by the areal capacitance of the gate dielectric at a given gate voltage in an identical device structure. At the same applied voltage, higher areal capacitance will attract more carriers at the dielectric/channel interface. The carrier transport is governed by percolation conduction over trap states and will be enhanced at high carrier concentrations by filling the trap states.[1a] Up to now, there are few reports discussing the solution-processed YO_x dielectric and its application in TFT devices.[17,21] All these reported literatures are based on organic-related species, and thus leading to a high annealing temperatures (>400 °C). This will undoubtedly restrict the integration of the TFTs on temperature-sensitive flexible electronics. Importantly, in this experiment, spin-coated YO_x dielectric was treated by a sequential process using moderate UV/ozone treatment and low-temperature annealing at 300 °C.

The obtained WI YO_x thin film exhibits amorphous structure and smooth surface with a small root-mean square value of 0.26 nm (see Figure S4, Supporting Information). The areal capacitance and leakage current density of the WI YO_x dielectric are shown in **Figure 6**a,b. The areal capacitance of the YO_x dielectric is 360 nF cm^{-2} at 20 Hz with a relative dielectric constant of 14.8. Although the areal capacitance decreases slightly as the frequency increases, the areal capacitance variation from 20 Hz to 100 kHz is less than 8%, indicating low defect density such as hydroxyl group or/and oxygen vacancies in the thin film.[22] This is undoubtedly beneficial to the dielectric properties of the thin film because the conduction paths in dielectrics are mainly caused by hydroxyl and grain boundaries.[23] For this reason, the capacitor exhibits relatively low leakage current density (≈10^{-9} A cm^{-2} at 1 MV cm^{-1}) with a dielectric breakdown electric field larger than 4 MV cm^{-1}.

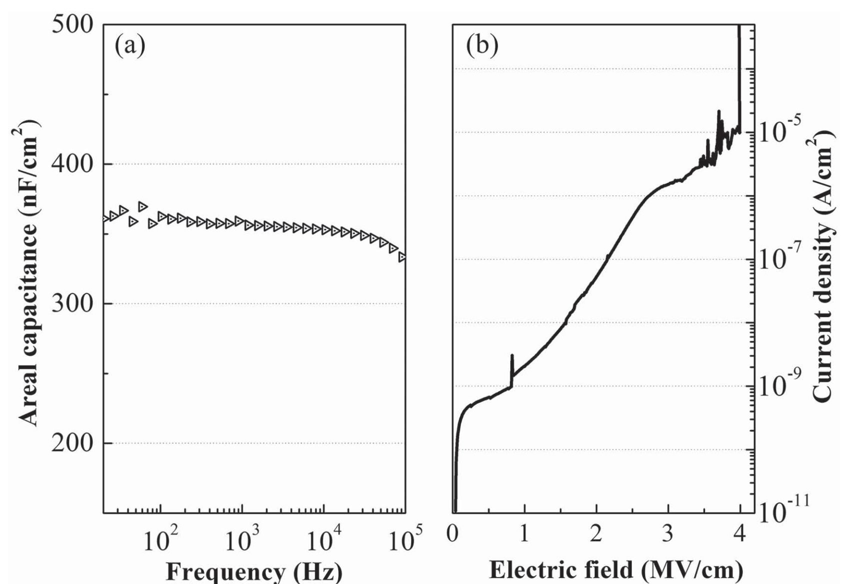

Figure 6. a) Areal capacitance and b) leakage current density of the YO_x dielectric.

2.7. Fully WI IZO TFT based on YO_x Dielectric

Figure 7a,b show the output and transfer curves of fully WI IZO/YO_x TFT. There it is also shown the hysteresis as well as the role of forward and reverse bias on the gate leakage current recorded. The as-fabricated TFT exhibits excellent electrical performance, including a high μ_{FE} of 25.9 cm^2 V^{-1} s^{-1}, a low V_{TH} of 0.23 V, an I_{on}/I_{off} of 4.5 × 10^7, a small subthreshold swing (SS) value of 65 mV dec^{-1}, as well as a small hysteresis of 0.08 V. Note that the SS value of 65 mV dec^{-1} is comparable to the theoretical SS value of 60 mV dec^{-1}. From SS we can infer the maximum density of surface state $\left(N_S^{max}\right)$ at the IZO/YO_x interface as[24]

$$N_S^{max} = \left[\frac{SS \times \log(e)}{kT/q} - 1\right]\frac{C_i}{q} \quad (4)$$

Taking into account the values of C_i and SS, N_S^{max} was calculated to be 3.7 × 10^{11} for fully WI IZO/YO_x TFT. This value is much lower than that of the oxide TFTs based on organic-synthetic YO_x dielectric (N_S^{max} = 2.74 × 10^{12} cm^{-2}) and other high-k dielectrics,[25] Such a small N_S^{max} value indicates an electronic-clean interface. Importantly, the transistor operated at a low operating voltage (±1.5 V). As a result, the fabricated transistor dissipates a much lower power than the conventional SiO_2-based IZO TFT, as shown in Figure 2. From the transfer curve, it is also found that the off-state current (I_{off}) increases with decreasing V_G. This is mainly due to the relatively narrow

© 2015 WILEY-VCH Verlag GmbH & Co. KGaA, Weinheim

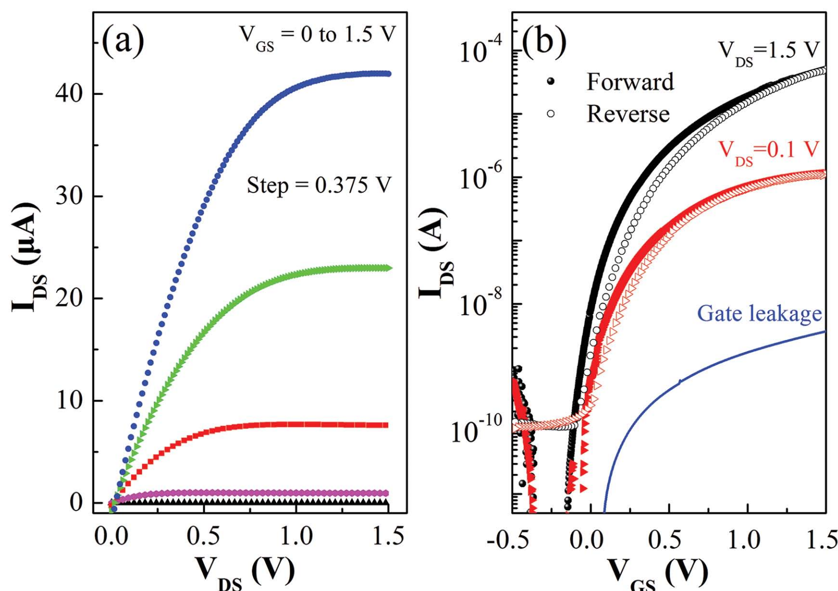

Figure 7. a) Output and b) transfer curves of fully WI IZO/YO_x TFT, showing the hysteresis behaviour observed when films are forward (full circles) and reverse bias (open circles).

bandgap (5.8 eV) of YO_x dielectric. The carriers can be easily injected into dielectric under an applied V_G, which will cause an increase in the I_{off}.[25b]

The high μ_{FE} at such a low operating voltage was undoubtedly beneficial from the smooth and dense YO_x dielectric due to the moderate UV/ozone treatment prior to thermal annealing process. UV/ozone treatment has been proved to be effective to decrease the decomposition temperature for oxide thin films and to improve the film roughness and surface energy.[4,26] The UV–vis absorption spectrum of precursor solution used for YO_x film preparation is shown in Figure S5, Supporting Information. In addition, the chemical corrosion to low-temperature-annealed dielectric, caused by organic-based channel precursor during spin-coating process, could be avoided due to the noncorrosive property of water solvent. This combination process improves the interface properties, which is important for TFT applications in terms of device performance and stability because the charge carriers always move along the interface between the semiconductor and the gate dielectric.

An important performance metric, particularly for low-temperature processed TFTs, is the operational device stability under bias stress. Here, a positive bias stress (PBS) test at V_G = 1.5 V and V_D = 1.5 V has been applied to the WI IZO/YO_x TFT for various time. The threshold voltage shift (ΔV_{TH}) in the transfer characteristics under PBS test is shown in **Figure 8**. For encapsulated WI IZO/YO_x TFT, the V_{TH} increased monotonically during stress, but only 0.22 V after 2 h. The parallel V_{TH} shift, without a change in the SS value, indicates that no additional defect states were created at the interface region under bias stressing. The interaction between the channel layer and oxygen in ambient atmosphere plays a critical role in determining the V_{TH} instability. When PBS test is applied in the atmosphere, the excess electrons were accumulated in the channel layer. The surrounding oxygen molecules have large electron negativity, which can capture electrons from the conduction band to form O^{2-} species. The adsorption of oxygen molecules in the channel layer can deplete the electron carriers, leading to a positive shift of V_{TH}.[14] This work is the first report discussing the electrical stability of the TFTs based on high-*k* YO_x dielectric. Further studies on WI oxide passivation layer will improve the overall performance of fully WI IZO/YO_x TFTs and are currently ongoing.[27] The excellent electrical performance of the IZO TFT based on WI YO_x indicates that fully water-inducement process is feasible to replace the conventional organic-based synthetic approach, which represents a significant step towards the development of nontoxic, low-cost, low-power consumption, and large-area oxide electronics.

3. Conclusions

In summary, we demonstrated a nontoxic and fully water-inducement route for oxide TFTs at low temperature. The TGA indicated dehydroxylation and oxide formation can be achieved at lower temperature by increasing the annealing time from 2 to 4 h. Amorphous IZO thin film was obtained upon being annealed at 230 °C. The optimized IZO TFT, annealed at 230 °C for 4 h, are activated, working in enhancement, with good device uniformity and electrical performance: μ_{FE} = 2.79 $cm^2\ V^{-1}\ s^{-1}$ and I_{on}/I_{off} = 6×10^7. Finally, the fully WI IZO/YO_x TFT was successfully integrated and the TFT showed high μ_{FE} of 25.9 $cm^2\ V^{-1}\ s^{-1}$

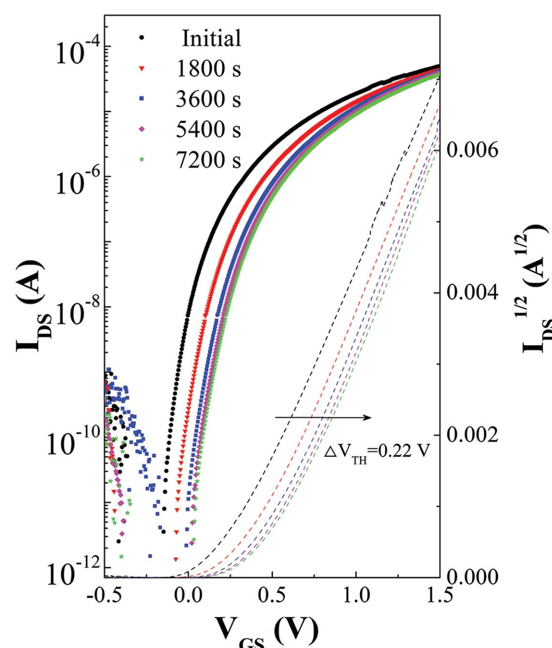

Figure 8. Variation of the transfer curves of IZO/YO_x TFT under PBS test for a duration of 2 h.

© 2015 WILEY-VCH Verlag GmbH & Co. KGaA, Weinheim

at ultralow operating voltage of 1.5 V. This novel nontoxic and fully water-inducement approach is highly expected to replace conventional organic-based synthetic route for fabricating low-temperature, high-performance, and flexible circuitry.

4. Experimental Section

Synthesis of Metal-Oxide Precursor Solutions: A quantity of 0.2 M $In(NO_3)_3 \cdot H_2O$ and $Zn(NO_3)_2 \cdot H_2O$ were dissolved in deionized (DI) water with a molar ratio of In:Zn = 7:3 to form the IZO precursor solution. A quantity of 0.2 M $In(NO_3)_3 \cdot H_2O$ was dissolved in DI water to form In_2O_3 precursor solution. YO_x solution was prepared by dissolving $Y(NO_3)_3 \cdot H_2O$ in DI water at a concentration of 0.15 M. All precursor solutions were stirred vigorously for 6 h under ambient conditions before spin-coating.

Fabrication of SiO_2-Based TFTs: A bottom-gate and top-contact structure was adopted for the TFT fabrication. Heavily doped p-type Si substrates with thermally grown SiO_2 gate dielectric (100 nm) were exposed under oxygen plasma (40 W) for 10 min to enhance the hydrophilicity before spin coating. The metal-oxide precursor solution was filtered through 0.2 μm syringe filter and then spun on SiO_2/Si substrates at 4500 rpm for 20 s. After that, the samples were annealed at various temperatures (200–300 °C) for various time intervals (0.5–5 h) in air. Finally, Al source and drain electrodes, with a thickness of 100 nm, were deposited on channel layers by thermal evaporation. The channel length and width were 250 and 1000 μm, respectively.

Fabrication of Fully WI TFTs: YO_x precursor solution was spun onto a P^+–Si substrate at 5000 rpm for 20 s and baked at 130 °C for 10 min. This procedure was repeated two times to obtain an appropriate thickness. The samples were then annealed by a sequential process using UV/ozone treatment for 40 min and thermal annealing at 300 °C for 100 min. The thickness of the formed YO_x thin film was measured to be 20 nm by using ellipsometry. The IZO precursor solution was then spun on YO_x/Si substrate at 4500 rpm for 20 s. The laminated thin films were annealed at 230 °C for 4 h. Finally, Al source and drain electrodes were deposited by thermal evaporation using the same shadow mask.

Supporting Information

Supporting Information is available from the Wiley Online Library or from the author.

Acknowledgements

This work was supported by the National Natural Science Foundation of China (Grant No. 51472130), Natural Science Foundation of Shandong Province (Grant Nos. ZR2011FM010 and ZR2012FM020). Y. Q. W. would like to thank the Taishan scholar program of Shandong Province for financial support.

Received: January 6, 2015
Revised: February 19, 2015
Published online: March 19, 2015

[1] a) K. Nomura, H. Ohta, A. Takagi, T. Kamiya, M. Hirano, H. Hosono, *Nature* **2004**, *432*, 488; b) E. Fortunato, P. Barquinha, R. Martins, *Adv. Mater.* **2012**, *24*, 2945; c) R. F. Martins, A. Ahnood, N. Correia, L. M. Pereira, R. Barros, P. M. Barquinha, R. Costa, I. M. Ferreira, A. Nathan, E. E. Fortunato, *Adv. Funct. Mater.* **2013**, *23*, 2153; d) M. G. Kim, M. G. Kanatzidis, A. Facchetti, T. J. Marks, *Nat. Mater.* **2011**, *10*, 382; e) K. Banger, Y. Yamashita, K. Mori, R. Peterson, T. Leedham, J. Rickard, H. Sirringhaus, *Nat. Mater.* **2010**, *10*, 45.

[2] a) Y. H. Hwang, J. S. Seo, J. M. Yun, H. Park, S. Yang, S. H. K. Park, B. S. Bae, *NPG Asia Mater.* **2013**, *5*, e45; b) E. Fortunato, P. Barquinha, A. Pimentel, L. Pereira, G. Goncalves, R. Martins, *Phys. Status Solidi (RRL)* **2007**, *1*, R34; c) E. Fortunato, P. Barquinha, G. Goncalves, L. Pereira, R. Martins, *Solid State Electron.* **2008**, *52*, 443; d) R. Branquinho, D. Salgueiro, L. Santos, P. Barquinha, L. Pereira, R. Martins , E. Fortunato, *ACS Appl. Mater. Interfaces* **2013**, *6*, 19592.

[3] J. W. Hennek, M. G. Kim, M. G. Kanatzidis, A. Facchetti, T. J. Marks, *J. Am. Chem. Soc.* **2012**, *134*, 9593.

[4] B. Y. Su, S. Y. Chu, Y. D. Juang, H. C. Chen, *Appl. Phys. Lett.* **2013**, *102*, 192101.

[5] a) S. T. Meyers, J. T. Anderson, C. M. Hung, J. Thompson, J. F. Wager, D. A. Keszler, *J. Am. Chem. Soc.* **2008**, *130*, 17603; b) S. YunáPark, Y. SangáKim, *RSC Adv.* **2014**, *4*, 11295.

[6] S. Oertel, M. P. Jank, E. Teuber, A. J. Bauer, L. Frey, *Thin Solid Films* **2014**, *553*, 114.

[7] T. Schneller, R. Waser, M. Kosec, D. Payne, *Chemical Solution Deposition of Functional Oxide Thin Films*, Springer, New York **2010**.

[8] Y. H. Lin, H. Faber, K. Zhao, Q. X. Wang, A. Amassian, M. Mclachlan, D. Anthopoulos, *Adv. Mater.* **2013**, *25*, 4340.

[9] J. H. Choi, S. M. Hwang, C. M. Lee, J. C. Kim, G. C. Park, J. Joo, J. H. Lim, *J. Cryst. Growth* **2011**, *326*, 175.

[10] S. Jeong, Y. G. Ha, J. Moon, A. Facchetti, T. J. Marks, *Adv. Mater.* **2010**, *22*, 1346.

[11] a) Y. H. Hwang, H. G. Im, H. Park, Y. Y. Nam, B. S. Bae, *ECS J. Solid State Sci. Technol.* **2013**, *2*, Q200; b)M. Niederberger, N. Pinna, *Metal Oxide Nanoparticles in Organic Solvents: Synthesis, Formation, Assembly and Application*, Springer, New York **2009**.

[12] a) L. Lu, Y. Miura, T. Nishida, M. Echizen, Y. Ishikawa, K. Uchiyama, Y. Uraoka, *Jpn. J. Appl. Phys.* **2012**, *51*, 03CB05; b) J. H. Park, Y. B. Yoo, K. H. Lee, W. S. Jang, J. Y. Oh, S. S. Chae, H. K. Baik, *ACS Appl. Mater. Interfaces* **2013**, *5*, 410.

[13] a) H.-K. Noh, J.-S. Park, K. J. Chang, *J. Appl. Phys.* **2013**, *113*, 063712; b) B. G. Son, S. Y. Je, H. J. Kim, C. K. Lee, C. K. Lee, A. Y. Hwang, J. Y. Won, J. H. Song, R. Choi, J. K. Jeong, *Phys. Status Solidi (RRL)* **2013**, *7*, 485.

[14] A. Liu, G. X. Liu, H. H. Zhu, F. Xu, E. Fortunato, R. Martins, F. K. Shan, *ACS Appl. Mater. Interfaces* **2014**, *6*, 17364.

[15] G. Adamopoulos, S. Thomas, P. H. Wöbkenberg, D. D. Bradley, M. A. McLachlan, T. D. Anthopoulos, *Adv. Mater.* **2011**, *23*, 1894.

[16] P. K. Nayak, M. Hedhili, D. Cha, H. Alshareef, *Appl. Phys. Lett.* **2013**, *103*, 033518.

[17] K. Song, W. Yang, Y. Jung, S. Jeong, J. Moon, *J. Mater. Chem.* **2012**, *22*, 21265.

[18] C. Avis, Y. G. Kim, J. Jang, *J. Mater. Chem.* **2012**, *22*, 17415.

[19] a) P. Barquinha, L. Pereira, G. Gonçalves, R. Martins, E. Fortunato, D. Kuscer, M. Kosec, A. Vilà, A. Olziersky, J. R. Morante, *J. Soc. Inf. Disp.* **2010**, *18*, 762; b) W. Yang, K. Song, Y. Jung, S. Jeong, J. Moon,*J. Mater. Chem. C* **2013**, *1*, 4275.

[20] Y. S. Rim, H. Chen, X. Kou, H. S. Duan, H. Zhou, M. Cai, H. J. Kim, Y. Yang, *Adv. Mater.* **2014**, *26*, 4273.

[21] a) G. Adamopoulos, S. Thomas, D. D. C. Bradley, M. A. McLachlan, T. D. Anthopoulos, *Appl. Phys. Lett.* **2011**, *98*, 123503; b) C. Y. Tsay, C. H. Cheng, Y. W. Wang, *Ceram. Int.* **2012**, *38*, 1677.

[22] J. H. Park, K. Kim, Y. B. Yoo, S. Y. Park, K. H. Lim, K. H. Lee, H. K. Baik, Y. S. Kim,*J. Mater. Chem. C* **2013**, *1*, 7166.

[23] J. Ko, J. Kim, S. Y. Park, E. Lee, K. Kim, K. H. Lim, Y. S. Kim,*J. Mater. Chem. C* **2014**, *2*, 1050.

© 2015 WILEY-VCH Verlag GmbH & Co. KGaA, Weinheim

[24] R. Martins, P. Barquinha, I. Ferreira, L. Pereira, G. Goncalves, E. Fortunato, *J. Appl. Phys.* **2007**, *101*, 044505.
[25] a) K. Song, W. Yang, Y. Jung, S. Jeong, J. Moon, *J. Mater. Chem.* **2012**, *22*, 21265; b) Y. G. Kim, C. Avis, J. Jang, *ECS Solid State Lett.* **2012**, *1*, Q23; c) K. M. Kim, C. W. Kim, J. S. Heo, H. Na, J. E. Lee, C. B. Park, J. U. Bae, C. D. Kim, M. Jun, Y. K. Hwang, *Appl. Phys. Lett.* **2011**, *99*, 242109; d) S. M. Hwang, S. M. Lee, J. H. Choi, J. H. Lim, J. Joo, *J. Nanosci. Nanotechnol.* **2013**, *13*, 7774.
[26] G. X. Liu, A. Liu, Y. Meng, F. K. Shan, B. C. Shin, W. J. Lee, C. R. Cho, *J. Nanosci. Nanotechnol.* **2015**, *15*, 2185.
[27] S. An, M. Mativenga, Y. Kim, J. Jang, *Appl. Phys. Lett.* **2014**, *105*, 053507.

© 2015 WILEY-VCH Verlag GmbH & Co. KGaA, Weinheim